JACS
JOURNAL OF THE AMERICAN CHEMICAL SOCIETY
Communication
pubs.acs.org/JACS

Nonequilibrium Hybridization Enables Discrimination of a Point Mutation within 5−40 °C

Maria Stancescu,[†] Tatiana A. Fedotova,[†] Jef Hooyberghs,[‡,∥] Alexander Balaeff,[§] and Dmitry M. Kolpashchikov*[,†,⊥]

[†]Chemistry Department, University of Central Florida, Orlando, Florida 32816, United States
[⊥]National Center for Forensic Science and Burnett School of Biomedical Sciences, University of Central Florida, Orlando, Florida 32816, United States
[‡]Flemish Institute for Technological Research, VITO, Boeretang 200, Mol B-2400, Belgium
[∥]Theoretical Physics, Hasselt University, Campus Diepenbeek, Agoralaan - Building D, Diepenbeek B-3590, Belgium
[§]NanoScience Technology Center, 12424 Research Parkway, Suite 400, Orlando, Florida 32826, United States

Supporting Information

ABSTRACT: Detection of point mutations and single nucleotide polymorphisms in DNA and RNA has a growing importance in biology, biotechnology, and medicine. For the application at hand, hybridization assays are often used. Traditionally, they differentiate point mutations only at elevated temperatures (>40 °C) and in narrow intervals (ΔT = 1−10 °C). The current study demonstrates that a specially designed multistranded DNA probe can differentiate point mutations in the range of 5−40 °C. This unprecedentedly broad ambient-temperature range is enabled by a controlled combination of (i) nonequilibrium hybridization conditions and (ii) a mismatch-induced increase of equilibration time in respect to that of a fully matched complex, which we dub "kinetic inversion".

Analysis of single nucleotide substitutions (SNS) has a growing importance in the diagnostics of genetic and infectious diseases, genome-wide association studies, forensics, and other applications.[1] Hybridization probes have been extensively used in SNS analysis.[2] The probes consist of nucleic acid oligomers of 15−25 nucleotides (or longer) that hybridize to DNA/RNA analytes containing an SNS site of interest (Figure 1A). The duplex is subsequently destabilized by heat to differentiate fully matched hybrids from the mismatched ones. However, these probes enable SNS differentiation only within a relatively narrow temperature range (ΔT), which is above the ambient range.[3] Therefore, expensive instrumentation, such as, e.g., qPCR thermocyclers with high-resolution melting capabilities, is required for heating and temperature control. Other approaches for SNS differentiation at ambient temperatures employ DNA-binding proteins, taking advantage of the differences in the 3D recognition of matched or mismatched base pairs.[4] Although these techniques are well-recognized and extensively used, they require protein production and storage as well as specific assay conditions to maintain protein activity, and thus potentially more resource intensive than hybridization-based assays. On the other hand, the development of hybridization probes with SNS selectivity at a broad ΔT downshifted to ambient temperatures would eliminate the need for specialized equipment and aid RNA analysis in living cells[5] and molecular diagnostics in instrument-free settings.[6] An active search for such hybridization probes is ongoing in the field.[7]

One approach uses a "molecular beacon" (MB) probe,[8] a fluorophore- and a quencher-conjugated DNA stem−loop structure (Figure 1B). When bound to a complementary DNA, the MB probe switches from the folded conformation with quenched fluorescence to extended, highly fluorescent conformation. Compared to linear probes, MB probes exhibit a broader ΔT and lower melting temperatures (T_m) of the MB−analyte complexes. The changes in T_m and ΔT result from the equilibrium shift from the associated state (AS) toward the dissociated state (DS), the latter is stabilized by the base pairing of the stem portion of the unbound MB probe.[8b,9] We further advanced the idea of broadening ΔT by conformational constraints through using a multicomponent X probe (Figure 1c).[10] In this study, we found that the X probe differentiates between the matched and mismatched analytes in the range of 5−40 °C, contrary to the predictions of equilibrium thermodynamics. This unprecedentedly broad differentiation range of the X probes results from the nonequilibrium operation mode and the "kinetic inversion" effect observed in this study for the first time.

The X probe consists of a universal MB (UMB) probe and two adapter DNA strands m and f. The three strands form a tetrameric complex with the analyte (Figure 1C).[7b] The sequences of the matched (**T_G**) and mismatched (**T_A**) analytes, as well as of the linear (**L1**) and the MB (**MB1**) probes were identical to those reported by Tsourkas et al.[9] Our goal was to compare directly the performance of the X probe with that of the linear and MB probes studied eralier.[9] A series of four X probes was designed to be fully complementary to **T_G**. All the X probes used the same universal MB probe (**UMB1**) and strand f (**X1-f** in Table S1), but differed in the length of the analyte-binding arm of strand m, which varied from 6 to 9 nucleotides (Table S1).

Received: June 9, 2016
Published: September 28, 2016

DOI: 10.1021/jacs.6b05628
J. Am. Chem. Soc. 2016, 138, 13465−13468

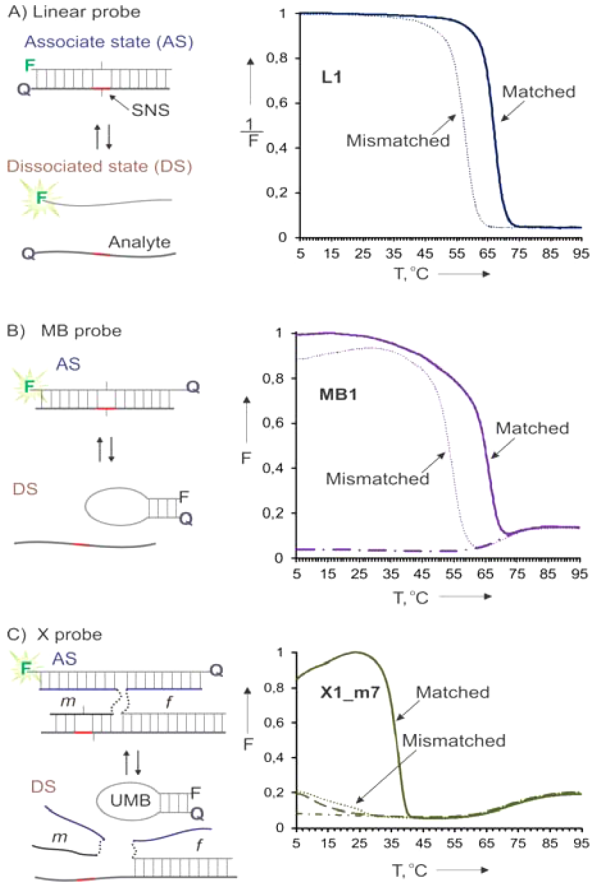

Figure 1. Three types of hybridization probes: designs and fluorescent melting profiles in the presence of the matched (solid line) or mismatched (dotted line) analytes. (A) Linear probe: an unfolded DNA probe hybridizes to a nucleic acid analyte. In the study, the analytes were labeled with a quencher dye (Q), whereas **L1** probe was labeled with a fluorophore (F). (B) Molecular beacon (MB) probe. The dash-dotted line (right panel) indicates the melting profile of the **MB1** alone. (C) X probe: strands m and f bind both the analyte and the universal MB (UMB) probe to form a four-stranded fluorescent complex (AS). Right panel: The melting profiles for the **X1_m7** (nonequilibrium conditions at low temperatures, see main text). The dash-dotted line, melting of **UMB1** alone; dashed line, melting of the **X1_m7**, no analyte. For experimental details, see Figure S1.

For **L1**, the difference in the probe–analyte T_m (ΔT_m), the commonly used characteristics of SNS differentiation efficiency, was 9.6 °C, which was identical to the value reported by Tsourkas et al.[9] (cf. Table S2 and Figure 1A). As expected, the ΔT_m for the **MB1** was broader (11.2 °C) and shifted by 2–3 °C toward lower values (Table S2), in agreement with the previous data.[9] For the X probes, however, the downshift of T_m by 30 °C and the broadening of the ΔT_m by 5–7 °C (in comparison with **L1** and **MB1** probes) were observed (Table S2). This performance exceeds that of other conformationally constrained probes.[8,11] We explained this effect by the greater stabilization of the DS for the X probe as compared to the **L1** or the **MB1** (Table S3, Figure S3, S4). The DS of the X probe is more stable than that of the MB probe due to (i) the residual hybrid between strand f and the analyte and (ii) higher entropy of the DS resulting from the complex dissociating into three rather than two fragments, as would be the case for the MB probe.

To visualize better the SNS differentiation of the three probes, we plotted the F_m/F_{mm} ratio as a function of temperature, where F_m and F_{mm} are the fluorescence intensities of the probes in the presence of matched and mismatched analytes, respectively (Figure 2A). The F_m/F_{mm} for the X probe

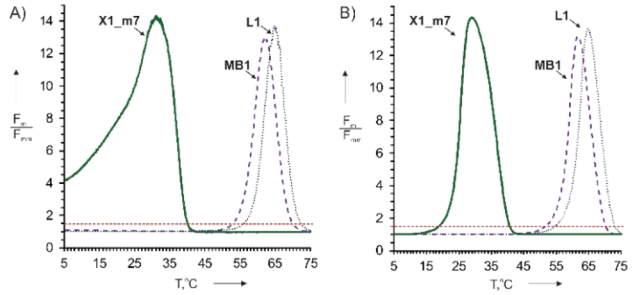

Figure 2. Discrimination profiles for the three hybridization probes. (A) The ratio of fluorescence produced by each probe in the presence of fully matched analyte (F_m) to that of mismatched analyte (F_{mm}) plotted against temperature for **L1** (dotted line), **MB1** (dashed line) and **X1_m7** (solid line). The threshold of $F_m/F_{mm} \sim 1.5$ is indicated by the red dotted line. (B) The nearest-neighbor (NN) model prediction of the profiles in the assumption of thermodynamic equilibrium (see SI for details).

was greater than 1 down to 5 °C (Figure 2A). Similar results were obtained for X probes with different lengths of m strands (cf. **X1_m6**, **8**, **9** in Figure S2) as well as at lower analyte concentrations (Figure S5). We describe this practically important property of the X probe by a new parameter, $\Delta T_{1.5}$, the temperature interval in which the fully matched analyte produces the signal 1.5 times greater than the mismatched analyte (Table S2).[12] The $\Delta T_{1.5}$ differentiation intervals were 14.8 and 17.1 °C for the **L1** and the **MB1** probes, respectively, and ca. 35 °C for the **X1_m7** probe (Figure 2 and Table S2). The discrimination curve for the **X1_m7** probe is asymmetric, with a SNS differentiation even at the temperatures below 15 °C (Figure 2A), which contradicts the theoretical curve predicted under the assumption of thermodynamic equilibrium (Figure 2B). These observation strongly suggest that the X-probe operated under nonequilibrium conditions at low temperatures.

To prove the latter point, we varied the heating and cooling rates in the hybridization experiments (Figure 3). The **MB1** probe reached equilibrium relatively fast, which is evident from the overlap of the fluorescent melting profiles obtained for the different equilibration times allowed for each 1 °C step of the cooling/heating cycle (Figure 3A). The fluoresecent signal profiles are nearly symmetric, reflecting that both cooling and heating bring the hybridization ensemble to the same equilibrium state. Furthermore, the equilibrium was reached at the cooling rate of 60 s/°C of the matched and 19 s/°C for the mismatched analyte (Figure 3C). Such hybridization kinetics is in agreement with the prior observations that mismatched duplexes equilibrate faster than the matched ones.[13] In contrast, the **X1_m7** probe demonstrated a strong hysteresis between the cooling and heating profiles (Figure 3B), indicating the absence of equilibrium. At 10 °C, the fluorescence of the fully matched **X1_m7**–analyte complex was somewhat stabilized[14] at the cooling rate of 60 s/°C (Figure 3D). For the mismatched analyte, however, the fluorescent signal kept monotonously increasing (Figure 3D) even when the equilibration time reached 16 h (Figure S6)

DOI: 10.1021/jacs.6b05628
J. Am. Chem. Soc. 2016, 138, 13465–13468

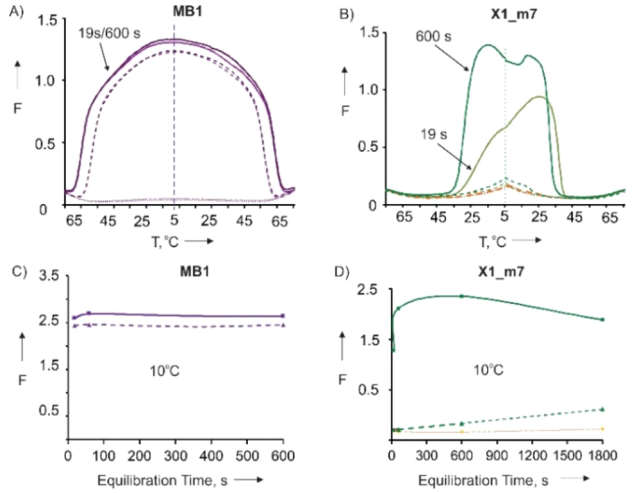

Figure 3. Equilibration of the probe–analyte complexes at different rates of the cooling–heating cycle. (A) Temperature dependence of the fluorescent signal for the **MB1** probe at the equilibration times of 19 or 600 s allowed per each 1 °C heating/cooling step. The solutions were first heated to 95 °C, then cooled to 5 °C, and then heated to 95 °C again. (B) Same as panel A for the **X1_m7** probe. (C) The fluorescent signal for the equilibration time of 19, 60, 600, or 1800 s/1 °C observed for the **MB1** probe–analyte complex at 10 °C during the cooling cycle. (D) Same as panel C for the **X1_m7** probe. The orange line corresponds to **X1_m7**, no analytes. Solid and dashed lines are used for the complexes of the probes with **T_G** (matched) or **T_A** (mismatched) analytes, respectively.

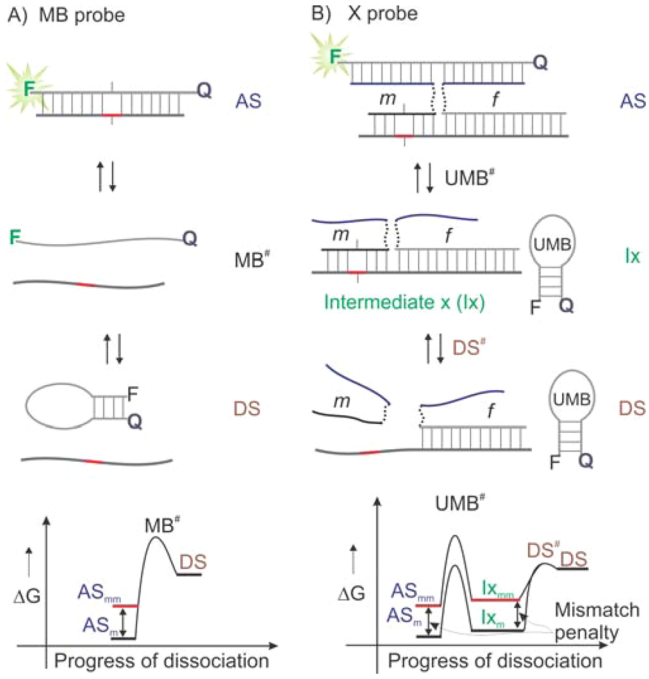

Figure 4. Hypothetical reaction diagrams for hybridization of (A) the MB probe and (B) the X probe at low temperatures. MB# and UMB# are the high energy random coil conformations with destabilized base-paring of the stem.[8b]

indicating that the probe–analyte hybridization remained incomplete. We therefore concluded that the complex of the **X1_m7** probe with the matched analyte equilibrated faster than with the mismatched analyte. To the best of our knowledge such a phenomenon, which we dub here "kinetic inversion", has not been previously reported. Kinetic inversion explains the broadening of the ΔT for the X probe toward lower temperatures: the lower the temperature, the more time is required for the equilibration, which effects the mismatched complex more than the matched one. To prove that the observed effect is not unique for a particular analyte sequence, we designed an X2 probe for the analysis of SNS in an arbitrary chosen DNA sequence of human RASSF1A gene (**T2_C** and **T2_T** in Table S1). The obtained melting profiles and ΔT differentiation range were similar to those observed for the X1 probe (Figure S7).

We explain the origin of the kinetic inversion phenomenon using the hybridization diagrams shown in Figure 4. For the MB probe–analyte complex, the AS formation can proceed via the transition state MB# wherein both the MB and the analyte strands presumably adopt random coil conformations.[8b] Thus, the AS formation is limited by the unfolding of the MB strand. The AS equilibration time, on the other hand, is determined by both the association (MB#→AS) and dissociation (AS→MB#) rates, and the latter is faster for the mismatched complex due to the lower activation energy. Thus, the MB probe equilibrates faster with mismatched than with matched analytes, in agreement with others'[13] and our own (Figure 3) observations. In contrast, the hybridization for the X probe proceeds presumably via one or several intermediate states. In Figure 4B, one possible intermediate (**Ix**) is shown as a complex of the m and f strands with the analyte. We assume that the equilibration rate for both matched and mismatched hybridization is limited by the rate of equilibration of AS ⇆ **Ix**. The rate of AS → **Ix** should be the same for both matched and mismatched complex, because it depends on the stability of UMB stem loop, which is the same in both cases. On the other hand, the **Ix** → AS rate depends also on the steady-state concentration of the **Ix** intermediate: $\text{Rate}_{\text{Ix}\rightarrow\text{AS}} = k_{\text{Ix}\rightarrow\text{AS}} \times [\textbf{Ix}] \times [\text{UMB}]$. The [**Ix**] should be greater for the matched than for the mismatched probe–analyte complex, considering that the latter is affected by the mismatch penalty. Thus, the rate of **Ix** →AS production, and the overall equilibration rate should be greater for the matched than for the mismatched complex. For other conceivable intermediate states, the argument remains similar. This explanation corresponds to the "kinetic proof-reading" model suggested by Hopfield[15] to explain the high accuracy of strongly but nonspecifically driven biochemical reactions (e.g., replication, protein synthesis).

In conclusion, we reported a novel phenomenon: the complex of the multicomponent X probe with mismatched analytes equilibrates slower than with matched analytes. To the best of our knowledge, this phenomenon was not observed for other hybridization probes. The kinetic inversion enables differentiation of a point mutation in DNA in an unprecedentedly broad temperature range of 5–40 °C. This phenomenon can be exploited for the design of hybridization probes with high mismatch selectivity at low temperatures, such as the X probe studied here. Such designs open the possibility of detecting point mutations in RNA in living cells and developing room-temperature diagnostic assays that operate without precise temperature control.

■ ASSOCIATED CONTENT

Supporting Information

The Supporting Information is available free of charge on the ACS Publications website at DOI: 10.1021/jacs.6b05628.

DOI: 10.1021/jacs.6b05628
J. Am. Chem. Soc. 2016, 138, 13465–13468

Details of experimental procedures, DNA sequences, computer modeling and probe design, fluorescent response of different X probes and phase diagrams fitting the thermodynamic parameter (PDF)

AUTHOR INFORMATION

Corresponding Author

*dmitry.kolpashchikov@ucf.edu

Notes

The authors declare no competing financial interest.

ACKNOWLEDGMENTS

We thank Dr. Yulia V. Gerasimova for helpful discussions. D.M.K. was funded by NSF CCF 1423219 and NIAID R15AI10388001A1. J.H. received funding from the Research Fund - Flanders (FWO K226314N). A.B. was supported by the UCF startup funds. The computational time for the project was provided by the UCF STOKES cluster.

REFERENCES

(1) Sudmant, P. H.; Rausch, T.; Gardner, E. J.; Handsaker, R. E.; Abyzov, A.; et al. *Nature* **2015**, *526*, 75−81.

(2) (a) Marras, S. A.; Tyagi, S.; Kramer, F. R. *Clin. Chim. Acta* **2006**, *363*, 48−60. (b) Kim, S.; Misra, A. *Annu. Rev. Biomed. Eng.* **2007**, *9*, 289−320. (c) Kolpashchikov, D. M. *Chem. Rev.* **2010**, *110*, 4709−4723. (d) Knez, K.; Spasic, D.; Janssen, K. P.; Lammertyn, J. *Analyst* **2014**, *139*, 353−370.

(3) (a) Lam, C. W.; Lau, K. C.; Tong, S. F. *Adv. Clin. Chem.* **2010**, *52*, 1−18. (b) Meaburn, E.; Butcher, L. M.; Schalkwyk, L. C.; Plomin, R. *Nucleic Acids Res.* **2006**, *34*, e27. (c) Hadiwikarta, W. W.; Van Dorst, B.; Hollanders, K.; Stuyver, L.; Carlon, E.; Hooyberghs, J. *Nucleic Acids Res.* **2013**, *41*, e173.

(4) (a) Olivier, M. *Mutat. Res., Fundam. Mol. Mech. Mutagen.* **2005**, *573*, 103−110. (b) Drabovich, A. P.; Krylov, S. N. *Anal. Chem.* **2006**, *78*, 2035−2038. (c) Gerasimova, Y. V.; Kolpashchikov, D. M. *Chem. Soc. Rev.* **2014**, *43*, 6405−6438. (d) Strerath, M.; Detmer, I.; Gaster, J.; Marx, A. *Methods Mol. Biol.* **2007**, *402*, 316−328.

(5) (a) Tyagi, S. *Nat. Methods* **2009**, *6*, 331−338. (b) Broude, N. E. *Mol. Microbiol.* **2011**, *80*, 1137−1147. (c) Armitage, B. A. *Curr. Opin. Chem. Biol.* **2011**, *15*, 806−812. (d) Urbinati, C. R.; Long, R. M. *Wiley Interdiscip. Rev. RNA* **2011**, *2*, 601−609.

(6) (a) Craw, P.; Balachandran, W. *Lab Chip* **2012**, *12*, 2469−2486. (b) Tong, Y.; Lemieux, B.; Kong, H. *BMC Biotechnol.* **2011**, *11*, 50.

(7) (a) Demidov, V. V.; Frank-Kamenetskii, M. D. *Trends Biochem. Sci.* **2004**, *29*, 62−71. (b) Kolpashchikov, D. M. *J. Am. Chem. Soc.* **2005**, *127*, 12442−12443. (c) Kolpashchikov, D. M. *ChemBioChem* **2007**, *8*, 2039−2042. (d) Kolpashchikov, D. M. *J. Am. Chem. Soc.* **2008**, *130*, 2934−1935. (e) Satterfield, B. C.; Bartosiewicz, M.; West, J. A.; Caplan, M. R. *J. Mol. Diagn.* **2010**, *12*, 359−367. (f) Gerasimova, Y. V.; Cornett, E.; Kolpashchikov, D. M. *ChemBioChem* **2010**, *11*, 811−817. (g) Kolpashchikov, D. M.; Gerasimova, Y. V.; Khan, M. S. *ChemBioChem* **2011**, *12*, 2564−2567. (h) Zhang, D. Y.; Chen, S. X.; Yin, P. *Nat. Chem.* **2012**, *4*, 208−214. (i) Chen, S. X.; Zhang, D. Y.; Seelig, G. *Nat. Chem.* **2013**, *5*, 782−789. (j) Abi, A.; Ferapontova, E. E. *Anal. Bioanal. Chem.* **2013**, *405*, 3693−3703. (k) Cornett, E. M.; O'Steen, M. R.; Kolpashchikov, D. M. *PLoS One* **2013**, *8*, e55919. (l) Kikuchi, N.; Kolpashchikov, D. M. *ChemBioChem* **2016**, *17*, 1589−1592.

(8) (a) Tyagi, S.; Kramer, F. R. *Nat. Biotechnol.* **1996**, *14*, 303−308. (b) Bonnet, G.; Tyagi, S.; Libchaber, A.; Kramer, F. R. *Proc. Natl. Acad. Sci. U. S. A.* **1999**, *96*, 6171−6176. (c) Kolpashchikov, D. M. *Scientifica* **2012**, *2012*, 928783.

(9) Tsourkas, A.; Behlke, M. A.; Bao, G. *Nucleic Acids Res.* **2002**, *30*, 4208−4215.

(10) (a) Kolpashchikov, D. M. *J. Am. Chem. Soc.* **2006**, *128*, 10625−10628. (b) Gerasimova, Y. V.; Hayson, A.; Ballantyne, J.; Kolpashchikov, D. M. *ChemBioChem* **2010**, *11*, 1762−1768. (c) Grimes, J.; Gerasimova, Y. V.; Kolpashchikov, D. M. *Angew. Chem., Int. Ed.* **2010**, *49*, 8950−8953. (d) Nguyen, C.; Grimes, J.; Gerasimova, Y. V.; Kolpashchikov, D. M. *Chem. - Eur. J.* **2011**, *17*, 13052−13058. (e) Gerasimova, Y. V.; Kolpashchikov, D. M. *Biosens. Bioelectron.* **2013**, *41*, 386−390.

(11) (a) Silvia, F.; Joana, B.; Pedro, M.; Ceu, F.; Jesper, W.; Filipe, A. N. *Appl. Microbiol. Biotechnol.* **2015**, *99*, 3961−3969. (b) Xiao, Y.; Plakos, K. J.; Lou, X.; White, R. J.; Qian, J.; Plaxco, K. W.; Soh, H. T. *Angew. Chem., Int. Ed.* **2009**, *48*, 4354−4358. (c) Kolpashchikov, D. M. *ChemBioChem* **2009**, *10*, 1443−1445.

(12) The 50% increase in the signal corresponds to the 3σ (99%) confidence interval, based on a typical standard deviation $\sigma \sim 15\%$ of the measured fluorescent output signal.

(13) (a) Wang, S.; Friedman, A. E.; Kool, E. T. *Biochemistry* **1995**, *34*, 9774−9784. (b) Dai, H.; Meyer, M.; Stepaniants, S.; Ziman, M.; Stoughton, R. *Nucleic Acids Res.* **2002**, *30*, e86. (c) Hooyberghs, J.; Baiesi, M.; Ferrantini, A.; Carlon, E. *Phys. Rev. E* **2010**, *81*, 012901. (d) Rauzan, B.; McMichael, E.; Cave, R.; Sevcik, L. R.; Ostrosky, K.; Whitman, E.; Stegemann, R.; Sinclair, A. L.; Serra, M. J.; Deckert, A. A. *Biochemistry* **2013**, *52*, 765−772.

(14) For solid line in Figure 3D, the increase in fluorescence within 900 s can be explained by continuous probe−analyte hybridization. The decrease of the signal between 900 and 1800 s is the result of the conformational adjustment of the fluorophore accompanied by the fluorescence quenching, as reported earlier (a) Nazarenko, I.; Pires, R.; Lowe, B.; Obaidy, M.; Rashtchian, A. *Nucl. Acids. Res.* **2002**, *30*, 2089−2195. (b) Lake, A.; Shang, S.; Kolpashchikov, D. M. *Angew. Chem., Int. Ed.* **2010**, *49*, 4459−4462.

(15) Hopfield, J. J. *Proc. Natl. Acad. Sci. U. S. A.* **1974**, *71*, 4135−4139.

DOI: 10.1021/jacs.6b05628
J. Am. Chem. Soc. 2016, 138, 13465−13468